Письма в ЭЧАЯ. 2015. Т. 12, № 6(197). С. 1204–1214

МЕТОДИКА ФИЗИЧЕСКОГО ЭКСПЕРИМЕНТА

BEAM TESTS OF CHERENKOV DETECTOR MODULES WITH PICOSECOND TIME RESOLUTION FOR START AND L0 TRIGGER DETECTORS OF MPD AND BM@N EXPERIMENTS

V. I. Yurevich [a, 1], *O. I. Batenkov* [b], *G. N. Agakishiev* [a], *G. S. Averichev* [a], *V. A. Babkin* [a], *S. N. Basylev* [a], *D. N. Bogoslovsky* [a], *L. G. Efimov* [a], *S. P. Lobastov* [a], *I. A. Philippov* [a], *A. A. Povtoreyko* [a], *V. Yu. Rogov* [a], *M. M. Rumyantsev* [a], *I. V. Slepnev* [a], *V. M. Slepnev* [a], *A. V. Shipunov* [a], *A. V. Terletsky* [a], *V. V. Tikhomirov* [a], *A. S. Veschikov* [b], *G. A. Yarigin* [a], *A. N. Zubarev* [a]

[a] Joint Institute for Nuclear Research, Dubna

[b] V. G. Khlopin Radium Institute, St. Petersburg, Russia

Two modular Cherenkov detectors FFD and T0 are developed for MPD and BM@N projects at LHEP, JINR for the study of Au + Au collisions. The aim of the detectors is the production of a start signal for a TOF detector and an effective L0 trigger for the collisions. The detector module design, characteristics, and results of tests with a deuteron beam are discussed. The time resolution of the modules for a single high-energy photon or charged hadron is $\sigma_t \approx 21-31$ ps and it depends on the method and electronics used.

Два модульных черенковских детектора — FFD и T0 — создаются для проектов MPD и BM@N в ЛФВЭ ОИЯИ для изучения Au + Au-столкновений. Назначением детекторов является производство стартового сигнала для TOF-детектора и эффективного L0-триггера столкновений. Обсуждаются конструкция, характеристики модулей детектора и результаты испытаний на пучке дейтронов. Временное разрешение модулей для высокоэнергетических одиночных фотонов или заряженных адронов составляет $\sigma_t \approx 21-31$ пс и зависит от используемого метода и электроники.

PACS: 29.40.Ka; 29.40.Gx

INTRODUCTION

The TOF measurement with picosecond time resolution and effective triggering nucleus–nucleus collisions with minimal background production are important features of any experiment in relativistic nuclear physics. Nowadays there are some experiments in operation and planning at RHIC, LHC, and NICA (under construction) colliders and fixed target experiments NA61 (SPS, CERN), HADES and CBM (SIS-100, GSI), BM@N (Nuclotron, JINR). The detectors solving the tasks of picosecond start signal for TOF and triggering collision events are an important part of these experimental setups.

[1] E-mail: yurevich@jinr.ru

About ten years ago a new large-scale project was started at JINR with a goal to design and create a world-class accelerator complex based on heavy-ion beams of booster, Nuclotron-M, and the NICA collider [1]. Parallel with the project, two large-scale experimental setups are prepared for studying nucleus–nucleus collisions, BM@N experiment with beams of Nuclotron-M at a maximum energy of 4.5 GeV per nucleon, and MPD experiment with Au beams of the NICA collider at $4 \leqslant s_{NN}^{1/2} \leqslant 11$ GeV [2, 3].

Responsibility of our group is also to start L0 trigger detectors, a T0 detector for BM@N, and a Fast Forward Detector (FFD) for MPD. The concept of FFD and the first experience obtained with a detector prototype were published in [4]. The concept is based on registration of Cherenkov radiation induced by high-energy photons from π^0-decays and relativistic charged pions produced in $\mathrm{Au} + \mathrm{Au}$ collisions. This must provide as excellent timing as effective selection of the collisions in a wide interval of impact parameter by L0 trigger.

In this paper, we describe our experience in developing and testing the detector modules for such detector arrays with picosecond time resolution.

1. MODULAR DETECTORS

The FFD and T0 detectors are designed as multichannel arrays where the main element is a detector module based on MCP-PMTs XP85012/A1-Q from Photonis. This device provides ps-timing, operation in strong magnetic field, and design of detector arrays with a small dead

Characteristics of multichannel detector arrays

Characteristics	Experiment, detector	
	MPD, FFD	BM@N, T0
Number of detector arrays	2	1
Number of modules	12×2	12
Number of channels	48×2	48
Required time resolution, ps	< 50	< 50
Min. bias triggering	Yes	Yes
Triggering central collisions	Yes	Yes
Operation in magnetic field B, T	0.5	0.5

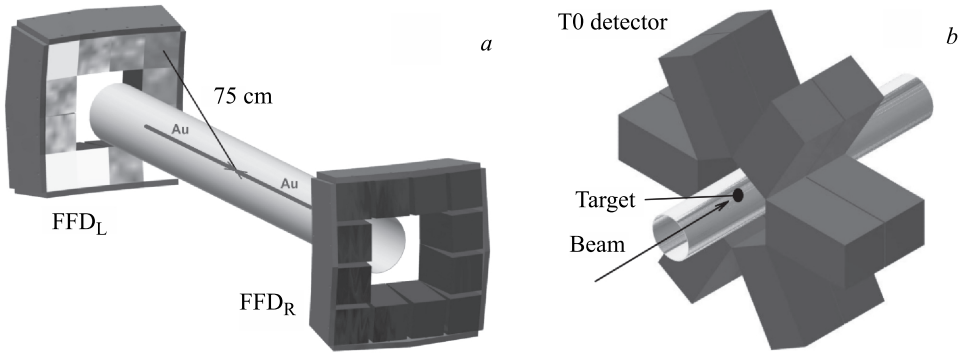

Fig. 1. Detector arrays: *a*) the FFD for MPD setup; *b*) the T0 detector for BM@N setup

area. The main characteristics of the detectors are given in the Table. The drawings of the FFD and T0 arrays are shown in Fig. 1.

The position of two arrays of the FFD is 75 cm from interaction point in the center of the MPD setup. These arrays cover a pseudorapidity range $2.3 < |\eta| < 3.1$. The 12 modules of the T0 detector are located around the vacuum pipe with a target in the center. The distance between the target position and the front surface of the modules is about 6 cm.

The detector performance was studied by MC simulation based on URQMD + GEANT3 and QGSM + GEANT4 codes. The efficiency of triggering Au + Au collisions in MPD and BM@N experiments via registration of high-energy photons and charged particles by the FFD and T0 arrays depends on centrality and corresponds to $\sim 100\%$ for a range of impact parameter $b < 10$ fm as is shown in Fig. 2.

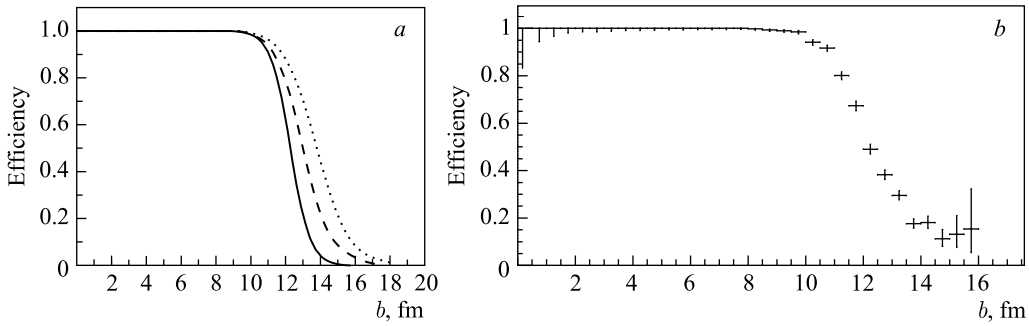

Fig. 2. Efficiency of registration of Au + Au collisions as a function of impact parameter: *a*) by the FFD with colliding nuclei at energy $s_{NN}^{1/2} = 5$ GeV for three cases — by a single FFD array (dashed curve), by two FFD arrays with a function OR (dotted curve), and a function AND (solid curve); *b*) by the T0 detector at a beam energy of $2A$ GeV

Since 2009 three versions of detector modules were designed, produced, and studied in test measurements with LED, cosmic rays, and deuteron/proton beams of the Nuclotron. In this paper, the results obtained in the last run with 3.5-GeV deuterons are discussed.

2. CHERENKOV DETECTOR MODULES

The detector module includes a lead plate of converter, a quartz radiator, MCP-PMT, a FEE board, a module housing, HV connector, signal SMA connectors, HDMI connector for LVDS signals, and LV for FEE as is shown in Fig. 3, *a*. The size of the module is $64 \times 64 \times 130$ mm. Four such modules prepared for study with a beam are shown in Fig. 3, *b*.

The incoming photons are converted to electrons in a 7-mm aluminum front panel of module housing and a lead plate 7–10 mm thick. The escaping electrons pass through a quartz radiator producing Cherenkov photons which are registered with UV-sensitive MCP-PMT XP85012/A1-Q. For test study with a beam we used a quartz radiator $59 \times 59 \times 15$ mm which covered all MCP-PMT front surface including a photocathode area 53×53 mm and a dead area over perimeter of MCP-PMT. The radiator consists of four equal bars $29.5 \times 29.5 \times 15$ mm each. All surfaces of the quartz bars were polished and the side surfaces were covered with

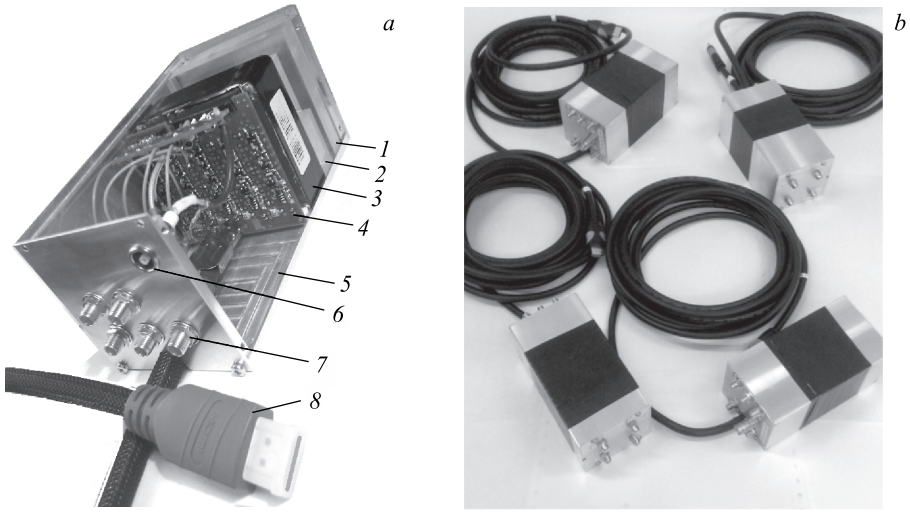

Fig. 3. *a*) FFD module content: *1* — the lead plate; *2* — the quartz radiator; *3* — the MCP-PMT; *4* — the FEE board; *5* — the module housing; *6* — the HV connector; *7* — the SMA connectors for analog signals; *8* — the HDMI connector for LVDS signals and LV; *b*) FFD modules prepared for tests with a beam

aluminized mylar. The MCP-PMT window adds 2 mm of quartz. The choice of thickness is a compromise between minimization of time jitter for Cherenkov photons arriving at the photocathode and increasing statistics of photoelectrons, that is important for good time resolution. Our choice is 17-mm thick quartz which is close to the optimum value and gives the best time resolution [5].

The number of quartz bars (2×2 bars per module) defines the granularity of the detector. The 8×8 anode pads of XP85012 are transformed into 2×2 cells by merging 4×4 pads of each cell into a single channel. Thus, each module has four independent channels plus one common signal from the second microchannel plate of MCP-PMT. The FEE board with five channels of a fast shaper-amplifier plus a discriminator sits directly on MCP-PMT connectors.

The amplification of pulses is split between MCP-PMT ($\sim 10^4 - 10^5$) and FEE amplifier (~ 50). Each channel of FEE produces the output analog pulse with a rise time of ~ 1.2 ns and a width of ~ 5 ns and the LVDS pulse which length depends on the pulse height. The output analog signals are transported through 50-Ohm SMA connectors and 2-m cables. The 5-m high-quality HDMI cable is applied for transport of all LVDS signals plus low voltages needed for FEE operation. The module operation is checked with a pulsed light source developed on the base of fast LED connected with optical fibers inserted into the module through the holes in the front surface.

The number of Cherenkov photons with wave lengths from λ_1 to λ_2 escaping in a radiator with length L and produced by a charged particle with $z = 1$ and $\beta = 1$ is calculated by the formula

$$N_{\mathrm{ph}} = 2\pi\alpha L \int\limits_{\lambda_1}^{\lambda_2} \left(1 - \frac{1}{n^2(\lambda)}\right) \frac{1}{\lambda^2} d\lambda. \tag{1}$$

As the time resolution depends on statistics of photoelectrons from a photocathode, one has to increase the photoelectron number as much as possible. The MCP-PMT XP82015/A1-Q has a good sensitivity in a wave length interval from 170 to 550 nm. In this region we get $N_{\rm ph} \approx 1800$ photons where about a half of this value lies in UV range $170 < \lambda < 270$ nm. Only a part of these photons produce the photoelectrons from photocathode, the loss is due to reflection, absorption, and low quantum efficiency of photocathode $QE \sim 20\%$.

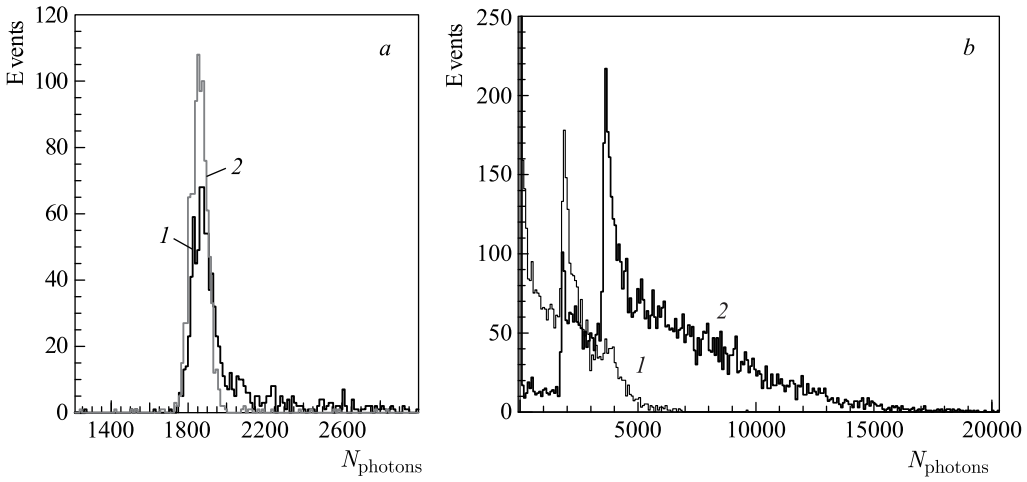

Fig. 4. Distribution of Cherenkov photon multiplicity in the quartz radiator induced by a single ultrarelativistic charged hadron (*1* — with a contribution from delta electrons, *2* — without this contribution) (*a*) and a single high-energy photon with energy of 50 MeV (*1*) and 500 MeV (*2*) (*b*)

Additionally, the Cherenkov photon multiplicity was studied with MC simulation. The obtained distributions for incoming single ultrarelativistic charged hadron and a high-energy photon with energy of 50 and 500 MeV are shown in Fig. 4, *a* and *b*, respectively. Here the thickness of the lead converter is 10 mm. In Fig. 4, *a*, the two distributions with a strong peak at $N_{\rm ph} \approx 1860$ photons are shown for charged hadrons, the solid curve presents the number of Cherenkov photons with contribution from delta electrons and the dashed curve, without this contribution. A high-energy photon can produce in the lead converter a single or several electrons which enter the quartz radiator and generate Cherenkov photons. It leads to a broad distribution with peaks from high-energy electrons passing through the quartz bar of the radiator. The first peak corresponds to the same position as the peak in Fig. 4, *a*. The second one corresponds to a pair of electrons which is much more intensive for 500-MeV photons than for 50-MeV photons where the first peak dominates. As one can see, the high-energy photons produce a much broader distribution of Cherenkov photon multiplicity than a single relativistic charged particle.

The MC simulation showed that the detection efficiency for photons depends on their energy, and for photons with energies 50, 100, 200, and 500 MeV the efficiency of detector module at a bias of 500 Cherenkov photons is 36, 56, 69, and 75%, respectively.

3. EXPERIMENTAL SETUP

The study of detector module performance was carried out with a 3.5-GeV deuteron beam of the Nuclotron at LHEP, JINR. The measurements were performed in 2013–2014 at a novel external beam channel specially created for test measurements with prototypes of sub-detectors of MPD and BM@N. The beam intensity varied from 10^3 to 10^5 deuterons per 2-s spill. A scheme and a photo of the experimental setup at the beam line are shown in Figs. 5 and 6, respectively.

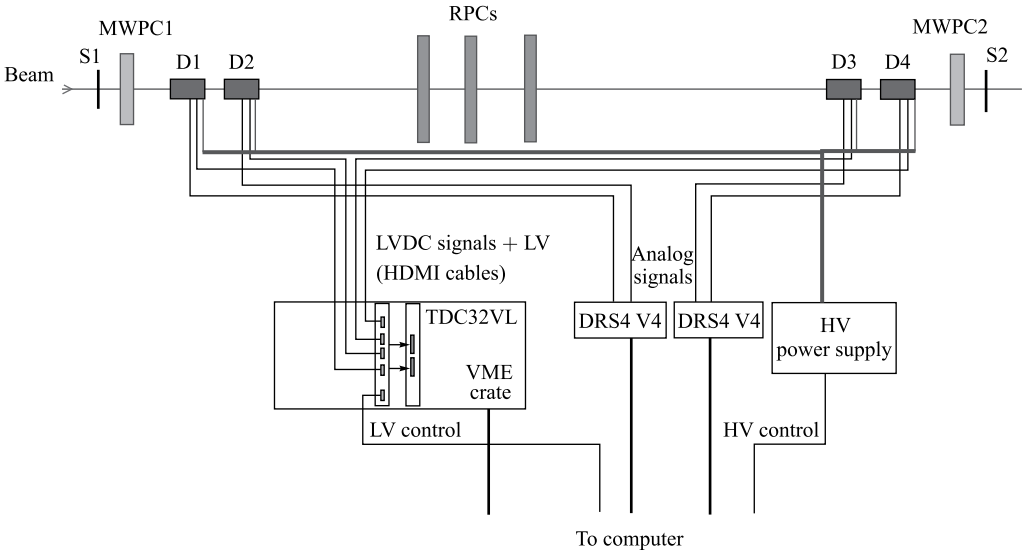

Fig. 5. Scheme of the experimental setup for study of detector modules: S1, S2 — the scintillation counters; MWPC1, MWPC2 — the multiwire proportional chambers; D1–D4 — the tested detector modules; RPCs — the resistive plate chambers of TOF detector

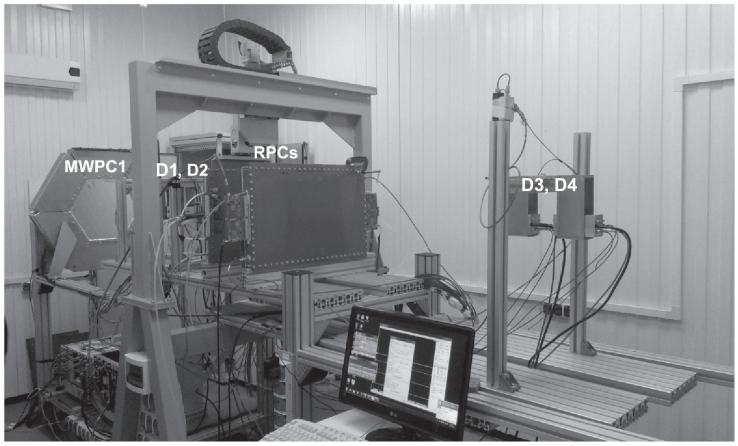

Fig. 6. Detector setup at the MPD test channel for the run with 3.5-GeV deuterons

Two pairs of detector modules were installed for the test along the beam axis. The modules did not contain lead converters. The first pair of modules D1 and D2 were placed behind the first MWPC, the second pair D3 and D4, at a distance of 2.7 m behind the first pair. The prototypes of RPCs of TOF detector were located in the middle of the experimental setup. The distance between the modules in the pairs was ~ 22 cm.

Two scintillation counters were used for trigger pulse production for each beam particle passing through the experimental area. The information from MWPCs was used for track reconstruction.

The LVDS signals from modules D1–D4 were fed via HDMI cables to a special board which aim was (i) production and control of low voltages for FEE and (ii) transport the LVDS signals to inputs of the VME module TDC32VL, 32-channel 25 ps multihit time stamping TDC [6].

The analog pulses were fed from the modules to two digitizers Evaluation Board DRS4 V4 designed at PSI [7]. This device is based on a DRS4 chip which is a switched capacitor array digitizing at sampling speed 5 GS/s that corresponds to 200-ps binning. It has SMA connectors for four input channels and USB 2.0 port for data readout, control, and power voltage.

Thus, two different readout methods were applied in the time-of-flight measurements for estimation of time resolution of the Cherenkov detector. In the first approach, used also for TOF RPC detectors, the LVDS signals were fed to TDC32VL modules. The length of LVDS pulses brings information about a pulse height used for time–pulse length correction in off-line analyses. The second method was digitizing form of the analog pulses. The rise time of the pulses after FEE corresponds to 6 time bins on the front slope of the pulses. It is enough for a good interpolation and finding t_0 position on the time scale in off-line analyses.

4. RESULTS OF TEST MEASUREMENTS WITH THE BEAM

In the measurements with DRS4 digitizer we studied (i) the form of pulses from analog outputs of detector modules, (ii) the pulse height distribution for beam particles hitting the back surface of the module, (iii) the cross talk response, and (iv) the time resolution of single detector channel.

Typical responses of the detectors D1–D4 are shown in Fig. 7 for ten events induced by 3.5-GeV deuterons. Here the deuteron tracks passed the central area of the quartz radiators. The rise time of pulses is 1.3 ns, the pulse width is 6 ns.

The rotation of detector by 180° leads to decreasing the pulse height by a factor of ~ 3. Thus, in a real experiment background particles will mostly give much smaller responses which can be rejected by a discriminator.

The measurements showed a small cross talk between the module channels with the negligible contribution to the detector responses.

The result of the TOF measurements with two pairs of detector modules is shown in Fig. 8. The linear fit of pulse front was used for t_0 finding for each detector pulse. The obtained TOF peaks are well approximated by Gaussian distribution with $\sigma \approx 33.5$ ps.

The beam velocity spread was less by a few ps and it gives a negligible contribution. The time jitter of the DRS4 digitizer increases with delay between pulses fed on different inputs and our estimation gives $\sigma_{\mathrm{DRS}} \approx 14$ ps for the test measurements with the beam. Taking into account these values, one can estimate the time resolution of the detector module $\sigma_t \approx 21.5$ ps.

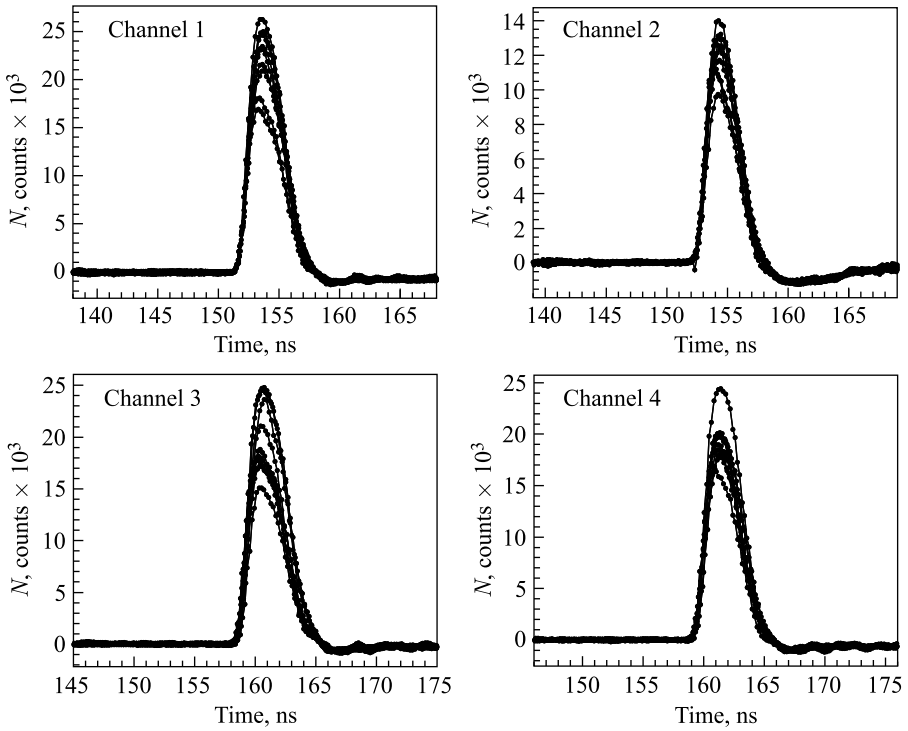

Fig. 7. Pulses of FFD modules for ten events measured with the digitizer Evaluation Board DRS4 V4

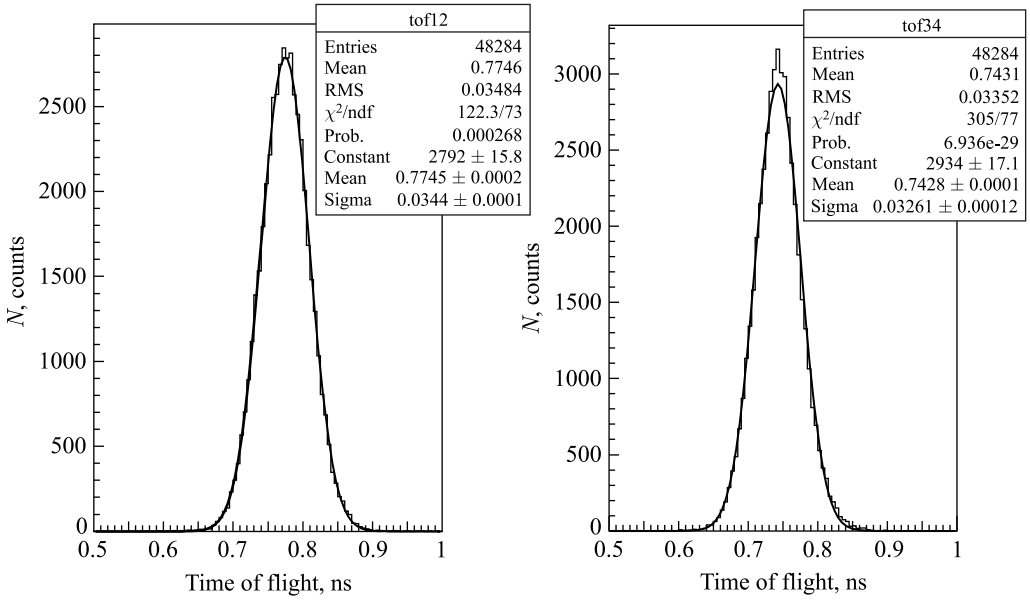

Fig. 8. TOF spectra obtained with the digitizer for individual channels of the detector pairs D1–D2 and D3–D4

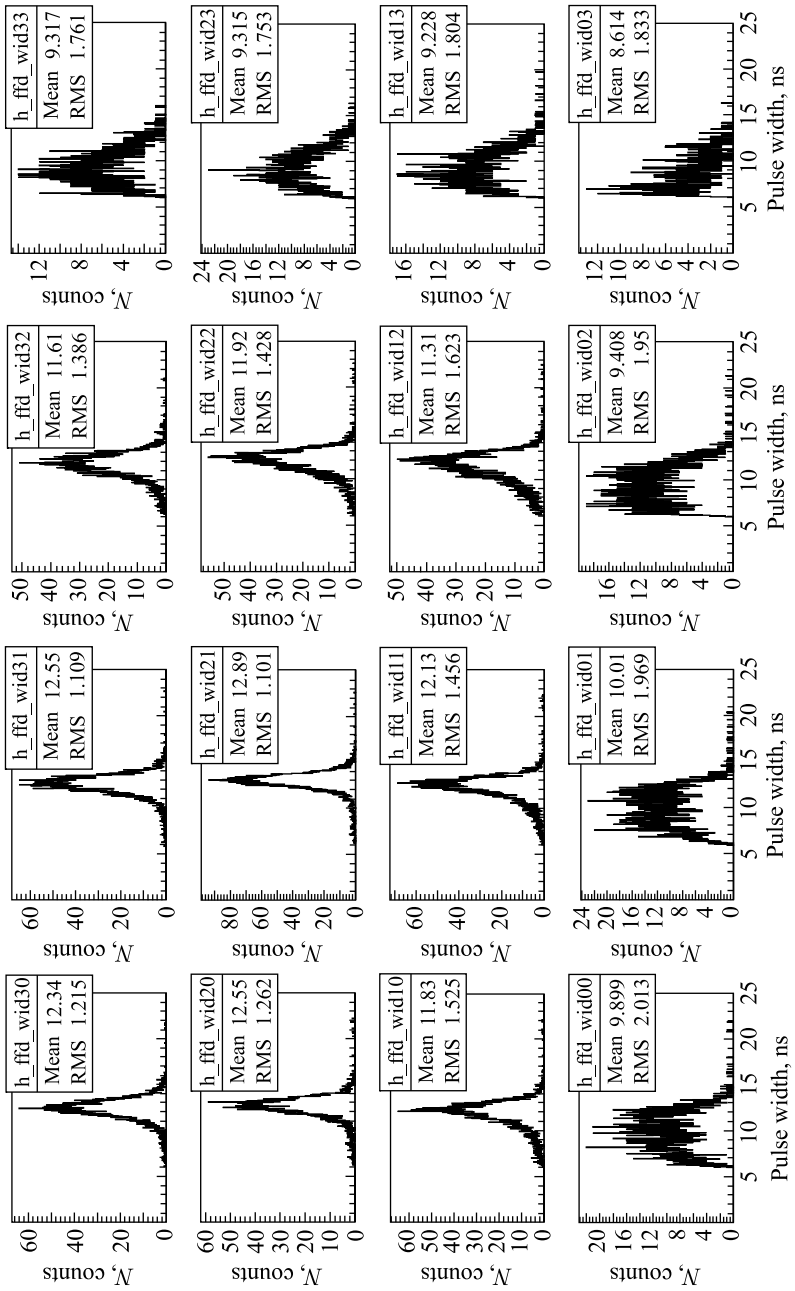

Fig. 9. Pulse width distributions of LVDS pulses for a single channel of the module for 4×4 virtual cells

Careful study of the dependence of the detector response on the position of deuteron track in the quartz radiator was carried out using the LVDS signals and the information about track position obtained with MWPCs. The cross section of a single quartz bar was split into 4×4 virtual cells of 7.4×7.4 mm. The pulse width distributions obtained for these cells are shown in Fig. 9.

Here the upper-left distribution corresponds to the center of MCP-PMT photocathode, the bottom and right rows correspond to the perimeter of MCP-PMT where the fraction of Cherenkov photons is lost in the dead area. The worst case is the result shown for the bottom-right corner where a lot of photons are lost in the dead area out of the photocathode. The shown results lead to the conclusion that for the central part of radiator, where the pulse width (amplitude) distribution is a rather narrow peak, one may expect to get much better time resolution. The time-of-flight results confirmed this expectation. For TOF peaks obtained with the LVDS signals, we got $\sigma \approx 50$, 62, and 80 ps for the central cells, the perimeter cells, and the bottom-right cell, respectively. This corresponds to $\sigma_t \approx 31$, 40, and 54 ps for the single detector after subtraction of the contribution of readout electronics.

Thus, one comes to the important conclusion that the extension of the radiator cross section up to total area of MCP-PMT XP85012 decreases the time resolution because of loosing an essential fraction of Cherenkov photons on the dead area of MCP-PMT. We decided to use the quartz radiator with cross section of 53×53 mm in the final version of the detector modules. Additionally, quality of polishing and aluminum layer on side surface of quartz bars will be improved to get better statistics of photoelectrons.

CONCLUSIONS

The beam tests showed that the developed modules of the FFD and T0 arrays provide the required time resolution $\sigma_t \approx 21-31$ ps and it depends on the method and readout electronics used.

The MC simulation showed that an ultrarelativistic single-charged particle produces about 1860 Cherenkov photons in a 17-mm quartz radiator in the wave length interval covered by XP85012. Also the simulation showed that the detector modules have high efficiency of registration of high-energy photons from 36% for 50-MeV photons to 75% for 500-MeV photons.

Nowadays we are ready for final production of the modules and the first 12 modules will be produced for the T0 detector with 10-mm lead converters and $53 \times 53 \times 15$ mm quartz radiators. Additionally, the quality of polishing and the aluminum layer on the side surface of quartz bars will be improved to get better statistics of the photoelectrons.

For study of Au + Au central collisions we expect to get with FFD or T0 detector much better time resolution. For these multihit events with N signals from the detectors, the resolution of start pulse is improved by a factor of $N^{1/2}$ and for the central collisions the estimation gives $\sigma_t < 10$ ps.

Acknowledgements. The authors are greatful to V. M. Golovatyuk, Yu. T. Kiryushin, and P. A. Rukoyatkin from JINR for help and assistance in the beam test and S. Ritt from PSI for help in application of Evaluation Board DRS4 in our measurements.

REFERENCES

1. *Sissakian A., Sorin A.* NICA Targets the Mixed Phase in Hadron Matter // CERN Courier. 2010. V. 50, No. 1. P. 13–15; http://nica.jinr.ru.
2. *Potrebenikov Yu.* Prospect for Dense Baryonic Matter at Nuclotron–NICA: BM@N and MPD Projects // Proc. of the 18th Intern. Seminar on High Energy Physics QUARKS-2014, Suzdal, Russia, 2014; http://quarks.inr.ac.ru.
3. *Zinchenko A.* Relativistic Heavy Ion Physics at JINR: Status of the BM@N and MPD Experiments // Proc. of the Particles and Nuclei Intern. Conf. PANIC'2014, Hamburg, Aug. 25–29, 2014.
4. *Yurevich V. I. et al.* Fast Forward Detector for MPD/NICA Project: Concept, Simulation, and Prototyping // Phys. Part. Nucl. Lett. 2013. V. 10, No. 3. P. 258–268.
5. *Va'vra J.* PID Techniques: Alternatives to RICH Methods. Report SLAC-PUB-14279. 2010.
6. http://afi.jinr.ru/TDC
7. http://www.psi.ch/drs/evaluation-board

Received on April 24, 2015.